AEROELASTIC STABILITY OF MODERN BEARINGLESS ROTORS - A PARAMETRIC INVESTIGATION

Khanh Q. Nguyen
Aerospace Engineer
NASA Ames Research Center
Moffett Field, CA

Abstract

The University of Maryland Advanced Rotorcraft Code (UMARC) is utilized to study the effects of blade design parameters on the aeroelastic stability of an isolated modern bearingless rotor blade in hover. The McDonnell Douglas Advanced Rotor Technology (MDART) Rotor is the baseline rotor investigated. Results indicate that kinematic pitch-lag coupling introduced through the control system geometry and the damping levels of the shear lag dampers strongly affect the hover inplane damping of the baseline rotor blade. Hub precone, pitchcase chordwise stiffness, and blade fundamental torsion frequency have small to moderate influence on the inplane damping, while blade pre-twist and placements of blade fundamental flapwise and chordwise frequencies have negligible effects. A damperless configuration with a leading edge pitch-link, 15 deg of pitch-link cant angle, and reduced pitch-link stiffness is shown to be stable with an inplane damping level in excess of 2.7 percent critical at the full hover tip speed.

Introduction

Ensuring aeromechanical stability is one of the primary requirements in the successful development of helicopter rotor systems. Aeromechanical instability such as air and ground resonance cause limit-cycle or divergent oscillations of the vehicle, resulting in catastrophic destruction of the vehicle or leading to fatigue failure of structural components. Aeromechanical stability is characterized by the coupling of the rotor inplane modes and the fuselage motions and depends largely on the damping level of the blade inplane mode. Therefore, the primary goal of this paper is to investigate the effects of blade design parameters on the aeroelastic stability (hub-fixed) of a modern bearingless main rotor in hover. The results of this investigation provide insights into the sources of inplane damping, identify key design parameters for improved inplane damping, and suggest viable damperless bearingless rotor configurations.

Bearingless rotors are characterized by flexural members that allow for blade flap, lead-lag, and pitch motions without discrete hinges or bearings. Early bearingless main rotors were designed without dampers and with either twin- or single-flexbeam and employ a pitchcase or torque tube for pitch changes. The blade inplane damping was often achieved with aeroelastic tailoring. In the past, the only two damperless bearingless rotor development programs that went through flight tests were a matched-stiffness rotor installed on the XH-51A helicopter (Ref. 1) and the Bearingless Main Rotor installed on the BO-105 airframe (Ref. 2). Modern bearingless rotors have evolved from several design processes and are included in current and planned future production helicopters worldwide. In particular, the Boeing-Sikorsky Comanche (Ref. 3), the McDonnell Douglas MD Explorer (Ref. 4), the Bell Helicopter 430 (Ref. 5), the Eurocopter Deutschland BO-108 (Ref. 6), and the Kawasaki OHX (Ref. 7) all employ modern bearingless rotor designs.

The major components of a modern bearingless main rotor are the blade, the single flexbeam, the pitchcase, and the snubber-damper assembly. The flexbeam is a flexural member that connects the blade to the hub, carries the centrifugal load, and allows for the blade flap, lead-lag, and twist motions. The pitchcase, a relatively rigid tube of elliptical cross-section, encloses the flexbeam, connects the blade to the control system through the pitch link, and serves to transfer the pitch inputs to the blade. The snubber acts as a pivot for the flap motions at the pitchcase inboard end and allows the pitchcase to rotate in pitch. The snubber also reacts the majority of the pitch link load and provides a load path for the pitchcase vertical and inplane shears to the hub. A pair of shear lag dampers, made of elastomeric materials, is mounted between the snubber and the pitchcase inboard end to augment the blade inplane damping. The snubber-damper assembly is a unique feature of modern bearingless rotors. The designs of the snubber-damper assembly in conjunction with the control geometry, the flexbeam, and the pitchcase dominate the aeroelastic characteristics of modern bearingless rotors.

For comparison purposes, the rotating-system inplane damping of three modern bearingless rotors in hover is shown in Fig. 1. The data were obtained from the full-scale tests of the McDonnell Douglas Advanced Rotor Technology or MDART rotor (Ref. 8) and the Sikorsky S-76 Bearingless Main Rotor or SBMR (Ref. 9) in the

Presented at the American Helicopter Society Aeromechanics Specialists Conference, San Francisco, CA, Jan. 19-21.

40- by 80-Foot Wind Tunnel, and an MBB bearingless rotor configuration (adapted from Fig. 31 of Ref. 10). The comparison shown in this figure clearly indicates the differences in the aeroelastic stability of the three rotor systems. The aeroelastic stability is expressed in terms of the decrement ratio, which is the product of the critical damping and the natural frequency in radian per sec of the blade fundamental inplane mode. For the collective pitch range above 4 deg, the damping of the MDART rotor increases faster than the damping of the other two rotors. At the collective pitch range below 4 deg, the damping levels of the MDART rotor and the MBB rotor are similar. The SBMR has significantly lower inplane damping than both the MDART and BO-108 rotors and exhibits a damping variation identical to that of the MBB rotor, probably reflecting a similar design philosophy. The difference in damping values between these two rotors is an almost uniform offset, probably due to the larger inertia of the SBMR blade. For a given shear lag damper, blades with larger mass moment of inertia about the virtual lag hinge have lower effective damping. The significance of the comparison shown in Fig. 1 is that certain blade design parameters create differences in the inplane damping variations among the three rotors. Identifying these design parameters improves the understanding of the aeroelastic stability behavior of modern bearingless rotors and is beneficial in the development of future bearingless rotors with superior aeroelastic stability characteristics.

Parametric investigations of blade design parameters on the aeromechanical stability of several bearingless rotor configurations are presented in Refs. 11-14. Ref. 11 presents the parametric results based on the Boeing ITR bearingless rotor. The study was conducted using FLAIR analysis. A parametric study using the DART analysis on the HARP rotor is presented in Ref. 12. Both studies indicate the strong influence of kinematic and elastic couplings on the aeromechanical stability of the bearingless rotors under investigation.

Experimental investigations of blade parameters on the aeromechanical stability of two scaled model rotors of modern bearingless rotor configuration are presented in Refs. 13 and 14. Test hardware allowed modification of the blade design parameters during the test programs. Test results indicate that the design changes aimed to improve the stability margin have negligible effects or are at variant to analytical results.

The objective of this paper is to analytically identify the parameters that affect the isolated aeroelastic stability of a modern bearingless rotor blade in hover, in particular, the blade design parameters that increase the stability margin, a crucial first step in the prevention of ground and air resonance. Design parameters investigated include shear lag damping values, pitch-link mounting strategies, hub precone and blade pre-twist, pitchcase chordwise bending stiffness, and blade fundamental frequency placements. Selected damperless configurations and the contribution of aerodynamics to the inplane damping are also considered. The MDART rotor blade is the baseline rotor blade used in this study. The analysis is conducted using the University of Maryland Advanced Rotorcraft Code - or UMARC (Ref. 15).

UMARC Analysis

UMARC is a finite element code capable of analyzing rotors with redundant load paths and includes advanced unsteady aerodynamics and vortex wake modeling. The blade is modeled as an elastic, isotropic Bernoulli-Euler beam, undergoing small strains and moderate deflections. The blade degrees-of-freedom include flap bending, lead-lag bending, elastic twist, and axial deflections. The finite element method based on Hamilton's principle is used to discretize the blade, flexbeam, and pitchcase into a number of beam elements. Each beam element has fifteen degrees-of-freedom and consists of two end nodes and three internal nodes. The six degrees-of-freedom at each end node are the displacements and slopes for the flap and lead-lag bending, and displacements for elastic twist and axial deflections. There are two internal nodes for the axial degree-of-freedom and one internal node for the elastic twist. The formulation of the blade governing equations is developed for nonuniform blades having pre-twist, pre-pitch, precone, and chordwise offsets from the blade pitch axis for the loci of the center-of-mass and aerodynamic center, and the tensile and elastic axes.

To model a modern bearingless rotor with dual load-path, the blade boundary conditions and the connectivity between beam elements are incorporated into UMARC. The blade and flexbeam form one load path connected to the hub, and the pitchcase forms another load path connecting the blade to the control system and the snubber-damper assembly. The flexbeam inboard end is cantilevered to the hub. The pitchcase root is restrained by the snubber-damper assembly and the pitch-link, both of which are modeled as discrete springs. Furthermore, the pair of shear lag dampers are modeled as a linear viscous damper. Structural damping is not included. At the blade-flexbeam-pitchcase connection, continuities of all the degrees-of-freedom at the end node of the three interfacing beam elements are imposed.

In this investigation, the airloads are calculated using a quasi-steady aerodynamic model. For the steady inflow calculation, Landgrebe's prescribed wake model is used. A modal reduction technique, based on a number of computed natural vibration modes, is used to reduce the number of blade degrees-of-freedom. The resulting modal equations are solved using a finite element in time method. The trim control settings are prescribed or are solved iteratively together with the blade responses for prescribed steady hub loads.

The aeroelastic stability calculation is based on the linearized blade equations about the trim values. Modal reduction is also applied to the linearized blade equations. The effects of inflow dynamics are not included. Since only hover is considered in this investigation, the resulting Jacobian (or the derivative of the blade equations in the first order form) contains constant coefficients. Hence, the stability of the system is determined directly from the eigenvalues of the Jacobian. Figure 2, adapted from Ref. 8, shows the correlation between the UMARC computed inplane damping for an isolated rotor blade and the mean test data obtained from the full-scale test of the MDART rotor in the NASA Ames 40- by 80-Foot Wind Tunnel. The correlation results provide a high level of confidence in the predictive capabilities of UMARC and indicate that an isolated blade model is sufficient for stability analysis. In a separate study performed by Sikorsky Aircraft, UMARC has also been shown to perform extremely well in the prediction of the aeroelastic stability of the SBMR (Ref. 9).

Results and Discussion

The parametric investigation is carried out first to identify the contribution of aerodynamics and shear lag damping on the hover aeroelastic stability of the MDART rotor. Then the blade design parameters are varied around the baseline values and include the shear lag damper sizing, pitch-lag coupling introduced through leading-edge and trailing-edge pitch-link mounting and pitch-link cant angle, hub precone and blade pre-twist, pitchcase chordwise bending stiffness, and placements of the blade fundamental torsion, flap, and lag frequencies. Based on the results of this parametric study, a design configuration with selected parameters that yield the highest stability margin is investigated with and without the use of shear lag dampers. The rotor rotational speed is fixed at the nominal value of 392 rpm. The aeroelastic stability calculation is performed in the rotating system, and hence the results are presented in terms of rotating system damping.

Contributions of Aerodynamics and Shear Lag Damper

Individual contributions of aerodynamics and the shear lag damper on the inplane damping of the MDART rotor blade are shown in Fig. 3. With the shear lag damper removed, the MDART rotor is slightly unstable in the collective pitch range from 1 to 2.5 deg. In general, the aerodynamic contribution alone is not sufficient to stabilize the rotor for the collective pitch range below 4 deg. The increase in the aerodynamic contribution to the inplane damping at the collective pitch above 4 deg is due to the increase in the favorable flap-lag and pitch-lag couplings with airloading at the higher pitch settings. Flap-lag coupling, which depends on the orientation of the principal axes of the flap and lag bending, allows the transfer of the highly damped out-of-plane aerodynamic damping to the blade chordwise motion. Pitch-lag coupling evolves from the chordwise Coriolis coupling resulting from the radial shortening effect of the blade flapping in response to the pitch change.

On the basis of the near uniform offset value between the baseline and the no damper curves in Fig. 3, the net effect of the lag damper is to raise the inplane damping by 2.5-3 percent critical. This fact is confirmed by considering the results with the aerodynamics turned off, showing only the damper contribution. For the collective pitch range below 4 deg, the shear lag dampers contribute to all the inplane damping. The variation of damper damping with collective pitch is mild and has a slight increase with increasing pitch change. These results indicate that for the baseline rotor, the lag dampers contribute to all the inplane damping at the low collective pitch range (below 4 deg) and the aerodynamic contribution is moderate and increases with collective for the collective pitch range above 4 deg.

Shear Lag Dampers

The influence of the shear lag damper sizing on the inplane damping is shown in Fig. 4. This variation is accomplished by multiplying the baseline damping value by 1.5, 0.5, and zero (which is the same as the damper off case shown in Fig. 3). For the MDART rotor, the baseline damping value is nominally 18.3 lb-sec/in per damper, corresponding to damper undergoing large motions/strains at the blade fundamental lead-lag frequency. The stiffness and damping characteristics of elastomeric dampers was shown to be nonlinear functions of frequency and amplitude of the damper strain levels (Ref. 16). The shear lag damper of the MDART rotor within the UMARC analysis are characterized simply with linear viscous damper and discrete spring models. The snubber stiffness values are kept constant during this parametric investigation. The uniform offsets among the four curves shown are identical and indicate that the effect of the shear lag damper values, which is proportional to the structural damping ratio, on the inplane damping is linear. Note that this conclusion is restricted to the simplified model of the shear lag damper used in this study.

Kinematic Pitch-Lag Coupling

Pitch-lag coupling has been identified in Refs. 10-14 as a dominant parameter affecting the aeroelastic stability of bearingless rotors. On the baseline rotor, the pitch-link is mounted vertically at the pitchcase trailing edge, and the snubber-damper assembly rotates in pitch together with the pitchcase inboard end. This geometric arrangement produces a kinematic pitch-lag coupling which is proportional to the pitch angle of the pitchcase inboard end. The pitchcase inboard end is restrained in the out-of-plane motion by the axially stiff snubber and the relatively rigid pitch-link. The fundamental torsion fre-

quency of the MDART rotor is 6.44 per rev. In essence, the pitchcase inboard end can undergo chordwise and axial motions, and lag, flap, and pitch rotations. When the pitch of the pitchcase inboard end is nose up, a lag back motion of the blade causes the pitchcase inboard end to move forward in the chordwise direction resulting in the lowering of the pitch-link and hence a nose up pitch. Lag back-nose up is defined as positive pitch-lag coupling. Mounting the pitch-link at the pitchcase leading edge produces negative pitch-lag coupling with nose up pitch.

Figure 5 shows the influence of these couplings on the inplane damping. The results with the pitch-lag coupling artificially set to zero (a physically unrealizable configuration) is also shown for comparison . Compared with the zero coupling case, the effect of positive pitch-lag coupling is to increase the inplane damping above 7 deg collective; below 7 deg collective, the damping is reduced. Negative pitch-lag coupling, on the other hand, has larger damping levels below 6 deg collective compared with the zero and positive coupling cases; for collectives greater than 6 deg, the damping of the negative coupling case is reduced from the zero and positive coupling damping cases. The damping level with negative pitch-lag coupling is roughly 4 percent critical and increases only slightly with increasing collective for the range of collective pitch shown.

Figure 5 also shows the results for the leading edge pitch-link configuration (negative pitch-lag coupling) with the shear lag dampers removed. This damperless configuration remains stable within the range of collective pitch shown with the damping level between 1.2 to 1.8 percent critical. The minimum damping location has been shifted from 0 deg (for the baseline configuration) to 8 deg collective pitch.

For the baseline rotor, the amount of pitch-lag coupling can be varied by inclining the pitch-link at an angle relative to the vertical. For the trailing edge pitch-link configuration, moving the bottom end of the pitch-link aft is defined as positive pitch-link inclination. This effect is demonstrated in Fig. 6, where it shows the inplane damping with 15 deg, -15 deg, and 0 deg (corresponding to the baseline configuration) pitch-link inclination. Introducing 15 deg of pitch-link inclination increases the pitch-lag coupling, leading to an increase in damping at the collective pitch ranges above 8 deg and below 2.5 deg and a small reduction in the mid-collective pitch range (2.5-8 deg collective). The effect of the -15 deg pitch-link inclination is to negate the pitch-lag coupling introduced by the pitchcase rotation as collective pitch is increased, resulting in a damping trend similar to that of the case with zero pitch-lag coupling shown in Fig. 5.

The snubber-damper support axis can be mounted at an inclination to the pitchcase vertical (minor) axis, providing another source of kinematic pitch-lag coupling. Analytically, modeling of the pitch-link inclination is identical to the modeling of the inclination of the snubber-damper support axis. Therefore, the results shown in Fig. 6 apply as well to that of the snubber-damper inclination.

Hub Precone and Blade Pre-twist

Precone introduces elastic pitch-lag coupling on rotor blades. Out-of-plane bending of the blade, depending on blade precone, creates a moment arm that allows the inplane force to twist the blade. The effects of hub precone on the inplane damping of an isolated bearingless rotor blade are shown in Fig. 7. The baseline rotor has 3 deg of precone which starts from the flexbeam-hub attachment location. The precone is then varied from 0 to 4.5 deg for this parametric investigation. The results in this figure indicate that reducing hub precone is beneficial at the collective pitch range above 3 deg. The influence of hub precone at the low collective pitch range is small.

The effects of blade pre-twist on the aeroelastic stability of bearingless rotor are also examined. Blade pre-twist influences the level of flap-lag coupling on rotor blades. The baseline rotor has -10 deg of blade pretwist (twist down from root to tip) outboard of the flexbeam-blade clevis. The blade twist is varied to -8 and -12 deg. The effects on the hover aeroelastic stability are found to be negligible and are not shown.

Pitchcase Chordwise Stiffness

The effective damping of the shear lag dampers depends on the relative chordwise stiffness of the snubber-damper assembly, chordwise stiffness of the pitchcase, and the chordwise stiffness distribution of the flexbeam. A stiff snubber-damper does not allow enough motion of the pitchcase inboard end for effective damping. For a soft pitchcase, the damper damping is not efficiently transferred to the blade (Refs. 7, 10, 12). This fact is demonstrated in Fig. 8, where the effects of doubling and halving the baseline value of the pitchcase chordwise stiffness are shown. Reducing the pitchcase chordwise stiffness reduces the damper effectiveness, while increasing the chordwise stiffness improves the damper effectiveness and increases the level of kinematic pitch-lag coupling of the rotor blade. Note that doubling or halving the pitchcase chordwise stiffness from the baseline value results in less than one percent change in the blade fundamental lag mode frequency.

Blade Fundamental Frequencies

The blade fundamental torsion frequency is varied by adjusting the pitch-link stiffness. In this investigation, the blade torsion frequency is varied from 5.4 per rev to 6.6 per rev, representing an upper limit in frequency placement with pitch-link stiffness variation. The baseline rotor is relatively stiff in torsion, with the funda-

mental torsion frequency at 6.44 per rev. The results shown in Fig. 9 indicate that reducing the pitch-link stiffness improves inplane damping only at the high collective pitch range (above 6 deg). This beneficial effect is due to the increase in the level of the kinematic pitch-lag coupling for torsionally soft blades. Increasing the pitch-link stiffness from the baseline value does not produce a significant change in the inplane damping, probably because of the relatively small change in the torsion frequencies of the two rotor blades.

The blade fundamental flap and lag frequencies are varied by scaling the flexbeam flapwise and chordwise stiffness distributed values, respectively, by a constant. Three cases are considered: increase lag frequency from 0.63 to 0.70 per rev, increase flap frequency from 1.054 to 1.095 per rev, and increase both lag and flap frequencies to 0.70 and 1.095 per rev, respectively. Figure 10 shows that the effects of flap and lag frequencies on the inplane damping of this bearingless rotor configuration are negligible.

Combined Effects of Selected Parameters

The blade design parameters having the potential to increase blade inplane damping are selected and combined in two configurations. The first configuration, labeled as *Case 1*, has a reduced pitch-link stiffness (torsion frequency of 5.4 per rev), leading edge pitch-link (negative pitch-lag coupling) with 15 deg of inclination (with leading edge pitch-link, positive inclination means that bottom end of pitch-link is moved forward). The shear lag dampers are then removed from this configuration, giving the second configuration *Case 2*. The latter configuration allows the feasibility study of a *damperless* bearingless configuration.

The inplane damping of these two configurations are shown in Fig. 11 together with the baseline rotor blade for comparison. *Case 1* rotor has significantly higher damping than the baseline rotor in the collective pitch range below 8 deg. The damping level is high at 0 deg collective and decreases slightly, reaching a minimum at around 6 deg collective. The damping level remains relatively flat from 6 to 8 deg collective and increases moderately at the higher collective pitch range. At 0 deg collective pitch, the inplane damping is more than twice the baseline value (5.4 percent versus 2.3 percent critical damping of the baseline rotor). The *damperless* configuration represented by *Case 2* is also stable over the complete range of collective pitch shown. The minimum damping levels at 8 deg collective pitch is 2.7 percent critical. At 0 deg collective the inplane damping is 4 percent critical and is almost double that of the baseline rotor blade.

Conclusions

A sensitivity study is conducted to investigate the effect of blade design parameters on the hover aeroelastic stability of an isolated modern bearingless rotor blade. The MDART rotor is the baseline rotor used in this study, and the analysis is performed using UMARC. For the baseline rotor blade, the shear lag damper contributes 2.5-3 percent critical damping to the blade inplane motion, and the aerodynamic contribution to the inplane damping is absent for collective pitch below 4 deg. The results of the sensitivity of the blade design parameters at the nominal rotor rpm indicate:

1. The effect of shear lag dampers on the inplane damping of bearingless rotor is linear.

2. Kinematic pitch-lag coupling, regardless of its source, has large effects on the inplane damping.
   - The positive pitch-lag coupling introduced by trailing edge pitch-link and rotating snubber-damper assembly is beneficial for stability at the high collective pitch range and is detrimental at the low collective pitch range. Mounting the pitch-link at the leading edge produces the opposite effects.
   - For the trailing edge pitch-link configuration, positive pitch-link inclination (bottom of pitch-link moved aft) increases damping in the low (below 2.5 deg) and the high collective pitch (above 7.5 deg) ranges. Negative pitch-link inclination negates the effects of pitch-lag coupling introduced by the rotation of the snubber-damper assembly and yields damping results similar to that with no pitch-lag coupling.

3. Hub precone has a moderate effect on the inplane damping. Reducing precone is slightly beneficial at the high collective pitch range. Blade pre-twist has a negligible effect on the inplane damping.

4. Increasing the pitchcase chordwise stiffness allows more damper motion due to blade lag motion, thereby increasing blade inplane damping.

5. Torsionally soft blades have higher damping at the high collective pitch range than torsionally stiff blades. Placements of the blade fundamental flap and lag frequencies have negligible effects on the inplane damping.

6. A blade configuration with torsionally soft blade and leading edge mounting pitch-link at 15 deg inclination (bottom end of pitch-link moved forward) has superior stability margin than the baseline rotor. Even with the lag dampers removed, this configuration is quite stable with a minimum inplane damping of 2.7 percent critical at 8 deg collective pitch.

References

1. Donham, R. E., Cardinal, S. V., and Sachs, I. B., "Ground and Air Resonance Characteristics of a Soft In-Plane Rigid Rotor System," *Journal of the American Helicopter Society*, Vol. 14 (4), Oct. 1969.
2. Harris, F. D., Cancio, P. A., and Dixon, P. G., "The Bearingless Main Rotor," Proceedings of the Third European Rotorcraft and Powered-Lift Aircraft Forum, Aix-en-Provence, France, Sept. 1977.
3. Norman, T. R., Cooper, C. R., Fredrickson, C. A., and Herter, J. R., "Full-Scale Wind Tunnel Evaluation of the Sikorsky Five-Bladed Bearingless Main Rotor," Proceedings of the American Helicopter Society 49th Annual Forum, St. Louis, MO, May 1993.
4. McNulty, M., Jacklin, S., and Lau, B., "A Full-Scale Test of the McDonnell Douglas Advanced Bearingless Rotor in the NASA Ames 40 X 80 Foot Wind Tunnel," Proceedings of the American Helicopter Society 49th Annual Forum, St. Louis, MO, May 1993.
5. Harvey, D. S., "Bell's 430 - A Design Based On Optimism," *Rotor & Wing*, Vol. 27 (12), Dec. 1993.
6. Huber, H. B. and Schick, C., "MBB's BO-108 Design and Development," Proceedings of the American Helicopter Society 46th Annual Forum, Washington, D. C., May 1990.
7. Ichihashi, T. and Bandoh, S., "Design, Fabrication and Testing of the Composite Bearingless Rotor System for Rotary-Wing Aircraft," Proceedings of the Eighteenth European Rotorcraft and Powered-Lift Aircraft Forum, Avignon, France, Sept. 1992.
8. Nguyen, K. Q., McNulty, M., Anand, V., and Lauzon, D., "Aeroelastic Stability of the McDonnell Douglas Advanced Bearingless Rotor," Proceedings of the American Helicopter Society 49th Annual Forum, St. Louis, MO, May 1993.
9. Wang, J. M., Duh, J., Fuh, J. S., and Kottapalli, S., "Stability of the Sikorsky S-76 Bearingless Main Rotor," Proceedings of the American Helicopter Society 49th Annual Forum, St. Louis, MO, May 1993.
10. Huber, H. B., "Will Rotor Hubs Lose Their Bearings? A Survey of Bearingless Main Rotor Development," Proceedings of the Eighteenth European Rotorcraft and Powered-Lift Aircraft Forum, Avignon, France, Sept. 1992.
11. Hooper, E. W., "Parametric Study of the Aeroelastic Stability of a Bearingless Rotor," presented at the Second Decennial Specialists Meeting on Rotorcraft Dynamics, Moffett Field, CA, Nov. 1984.
12. Sorensen, J. L., Silverthorn, L. J., and Maier, T. H., "Dynamic Characteristics of Advanced Bearingless Rotors at McDonnell Douglas Helicopter Company," Proceedings of the American Helicopter Society 44th Annual Forum, Washington, D. C., Jun. 1988.
13. Weller, W. H. and Peterson, R. L., "Inplane Stability Characteristics for an Advanced Bearingless Main Rotor Model," *Journal of the American Helicopter Society*, Vol. 29 (3), Jul. 1994.
14. Weller, W. H., "Variation in Hover Aeromechanical Stability Trends with Bearingless Main Rotor Design," Proceedings of the American Helicopter Society 47th Annual Forum, Phoenix, AZ, May 1991.
15. Bir, G. S., Chopra, I., and Nguyen, K. Q., "Development of UMARC (University of Maryland Advanced Rotorcraft Code)," Proceedings of the American Helicopter Society 46th Annual Forum, Washington, D. C., May 1990.
16. Felker, F. F., Lau, B. H., McLaughlin, S., Johnson, W., "Nonlinear Behavior of an Elastomeric Damper Undergoing Dual-Frequency Motion and Its Effect on Rotor Dynamics," *Journal of the American Helicopter Society*, Vol. 34 (4), Oct. 1987.

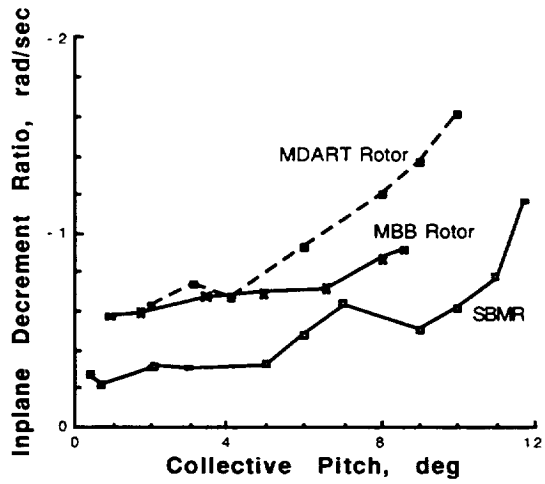

Fig. 1. Comparison of hover aeroelastic stability of three modern bearingless rotors.

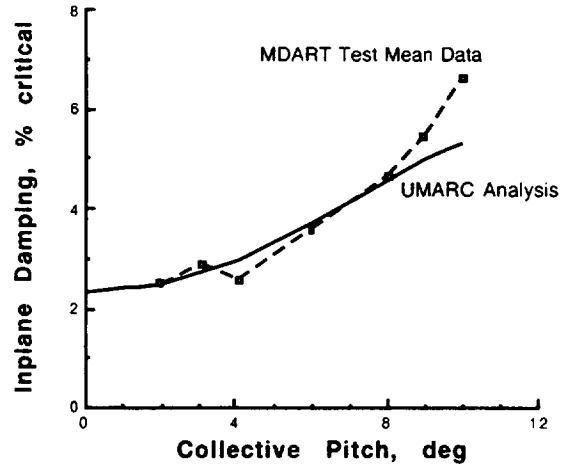

Fig. 2. Correlation of UMARC isolated blade results with MDART measured inplane damping in hover.

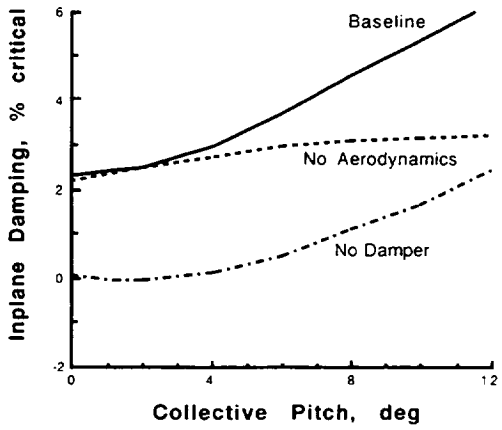

Fig. 3. Contributions of aerodynamics and dampers damping to inplane damping.

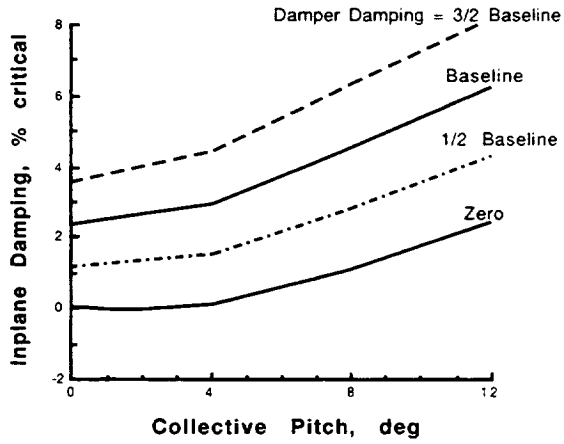

Fig. 4. Effects of the damping levels of shear lag dampers on inplane damping.

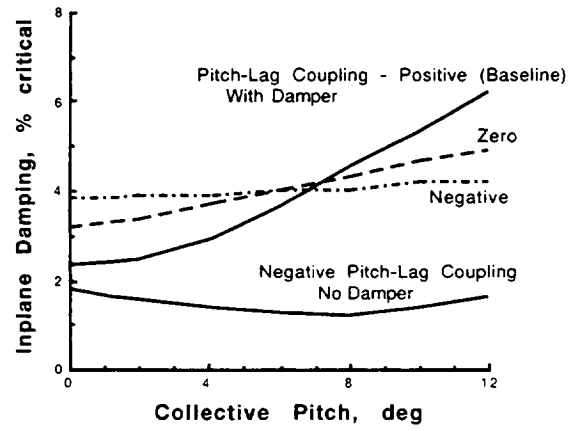

Fig. 5. Effects of leading edge and trailing edge pitch-link and removing the dampers on inplane damping.

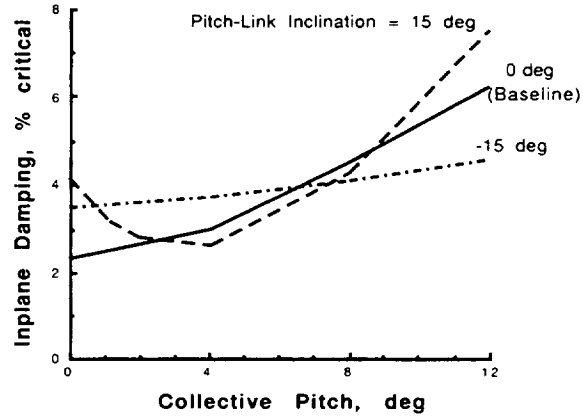

Fig. 6. Effects of pitch-link inclination on inplane damping.

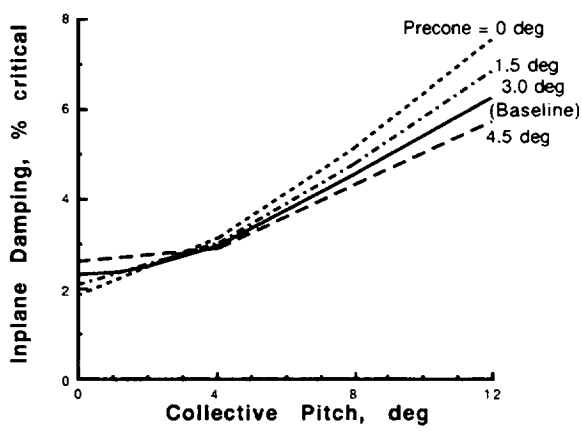

Fig. 7. Effects of hub precone on inplane damping.

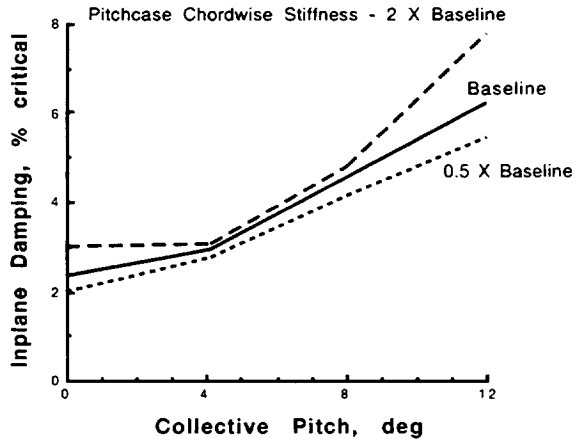

Fig. 8. Effects pitchcase chordwise stiffness on inplane damping.

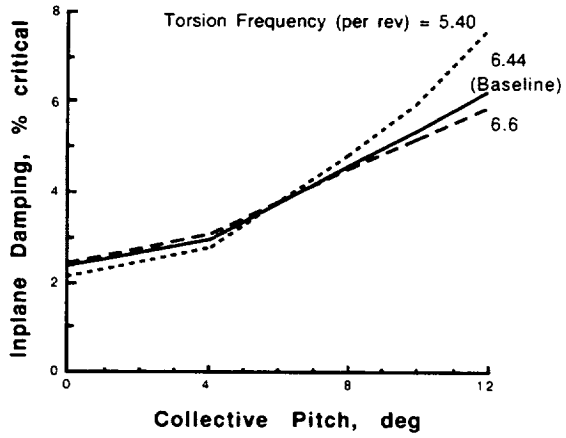

Fig. 9. Effects of blade torsion frequency on inplane damping.

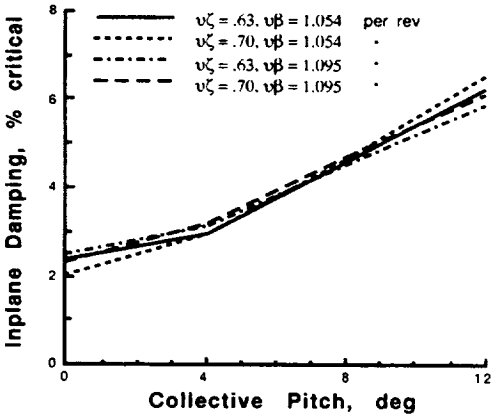

Fig. 10. Effects of fundamental lag and flap frequencies (υζ, υβ, respectively, per rev) on inplane damping.

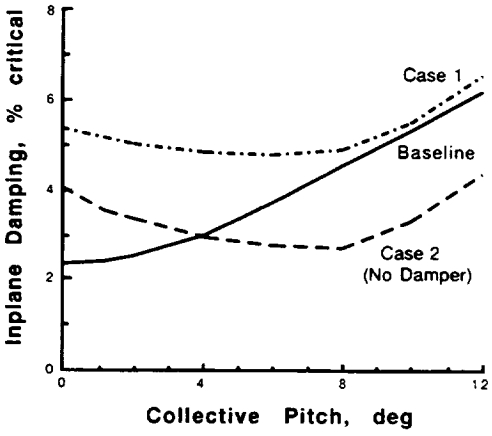

Fig. 11. Effects of combined parameters effects on inplane damping.